HIGH MASS FLUX TRANSPORT IN FLUIDS

John M. Kincaid

Department of Mechanical Engineering
SUNY at Stony Brook, Stony Brook, New York 11794-2300

Keywords: model, diffusion coefficient, self diffusion, molecular dynamics, Fick's Law, generalized hydrodynamics

ABSTRACT

A nonequilibrium molecular dynamics study of self diffusion in a Lennard-Jones-like fluid shows that the high mass-flux stages of mixing are described well by generalized hydrodynamics. There is no indication of the damped-wave propagation implied by the Telegrapher's equation, and the mass flux is less than that predicted by the diffusion equation.

INTRODUCTION

In this paper we examine, using the method of molecular dynamics, a simple fluid system that is, in a hydrodynamic sense, far from equilibrium, in particular a diffusive system in which the mass flux is so large that the diffusion equation (and Fick's Law) is not expected to provide an accurate description. Interest in 'correcting' the diffusion equation extends as far back as 1867 to Maxwell (who suggested that a damped wave equation should replace the diffusion equation) [1] and continues to recent work in the areas of generalized hydrodynamics [2,3], and extended irreversible thermodynamics [4]. The results of the nonequilibrium molecular dynamics simulations presented here provide some measure of clarification pertaining to the very earliest stages of the mixing process, and tend to support our earlier conclusion [3] that generalized hydrodynamics is the preferred description.

We begin by describing how a 'rectangular pulse' decays by self-diffusion in a moderately dense, Lennard-Jones-like, fluid at a moderate temperature, in d=2 and d=3 dimensions using the method of nonequilibrium molecular dynamics. We then briefly review several of the theories mentioned above and discuss the extent to which they describe the simulation results. We find that : (1) the simulated system behaves qualitatively, in many respects, like a system described by the classical diffusion equation; (2) there is no indication that the initial 'rectangular pulse' propagates as a wave (damped or undamped); and (3) that a simple modification of the usual generalized hydrodynamic approach provides a very accurate description of the simulation.

NONEQUILIBRIUM MOLECULAR DYNAMICS OF SELF DIFFUSION

The nonequilibrium molecular dynamics calculations were made for systems of particles that interact through the Lennard-Jones-spline potential [5]. This potential is a finite-ranged modification of the 12-6 Lennard-Jones potential. N particles were placed in a volume $V = L_x L_p^{d-1}$. Three such systems were examined: (1) d=3, $n\sigma^3 = 0.5$, $L_p/L_x = 6$; (2) d=3, $n\sigma^3 = 0.2$, $L_p/L_x = 6$; and (3) d=2, $n\sigma^2 = 0.5$, $L_p/L_x = 100$. In all cases initial states were selected from an ensemble of constant-energy, zero-momentum, molecular dynamics trajectories. The total energy was set so that $\langle k_B T/\varepsilon \rangle_{MD} = 2$ and periodic boundary conditions were used.. At time t = 0 all particles in a slab, perpendicular to the x axis and centered about x=0, were assigned a species label 1; the particles outside this slab were assigned species label 2; the slab width was $L_x/10$. The trajectory of the system was advanced using the Verlet algorithm; the integration time step was $0.003\ \sigma(m/\varepsilon)^{1/2}$ for d=3 calculations and $0.0025\ \sigma(m/\varepsilon)^{1/2}$ for the d=2 calculations. Every 30 time steps the number of species 1 and 2 particles in layers perpendicular to the x-axis were calculated (100 and 200 layers were used for d=3 and d=2 systems, respectively). The average 2nd, 4th, 6th, 8th, and 10th moments of the single-particle displacement, d(t), were also calculated.

To characterize the early stages of diffusion the d=3 trajectories were advanced 900 time steps and d=2 trajectories for 1200 time steps. The mole-fraction of species 1, c(x,t), was obtained by taking averages over an ensemble of N_I initial states. For the case d=3, $n\sigma^3=0.5$, $N_I = 92$; for d=3, $n\sigma^3=0.2$, $N_I = 100$; and for d=2, $n\sigma^2=0.5$, $N_I = 104$.

In Fig. 1 we plot c(x,t) as a function of x for several values of t for the case d=3, $n\sigma^3=0.5$; the c(x,t) for the other two cases are quite similar in form. c(x,t) has been

calculated for a discrete set of x-values corresponding to the x-coordinate of the center of a layer; we have displayed the piecewise continuous curve obtained by drawing a straight line between adjacent points. (A statistical analysis of all quantities given in this paper was performed using the methods described in Ref [6].) A few error bars having a total length of two standard deviations of the mean are placed on the curves to give a general impression of the statistical certainty of the results. In a qualitative sense c(x,t) looks remarkably 'diffusive' in character. However, we will see below that the c(x,t) are not the solutions of the diffusion equation.

The cumulants of the single-particle displacement, ρ_i (i=1,...5) were calculated from the moments of d(t). $\rho_1(t) = \langle d(t)^2\rangle/2!$, $\rho_2(t) = [\langle d(t)^4\rangle - 3\langle d(t)^2\rangle^2]/4!$, etc...., where the average is over the ensemble of trajectories. The ratios $\rho_i(t)/\rho_1(t)^i$ are zero at t = 0, reach a maximum and then decay to zero as $t \rightarrow \infty$ [7]. For i = 2 the ratio never exceeds 0.05, and for $i \geq 3$ the ratios are always less than 0.005.

THEORETICAL MODELS

In this section we compare the solutions of the diffusion equation, a damped wave equation, and a form of generalized hydrodynamics to the simulation results. Only the latter theory gives an adequate description.

The diffusion equation.

The classical diffuison equation of hydrodynamics is obtained by combining Fick's Law, $j_1(x,t) = - D\partial c(x,t)/ \partial x$, with the continuity equation, $\partial c(x,t)/ \partial t = - \partial j_1(x,t)/ \partial x$:

$$\frac{\partial c_{DE}(x,t)}{\partial t} = D\frac{\partial^2 c_{DE}(x,t)}{\partial x^2} \quad . \tag{1}$$

Here j_1 is the number flux of species 1 and D is the self-diffusion coefficient. D depends on T and n but is independent of $c_{DE}(x,t)$ [2]. D has been calculated by Kincaid et al.[6] for the three-dimensional states considered here. [$D = 0.412\ \sigma(\varepsilon/m)^{1/2}$, $n\sigma^3 = 0.5$; $D = 1.30\ \sigma(\varepsilon/m)^{1/2}$, $n\sigma^3 = 0.2$.] Given the rectangular pulse initial condition, c(x,0), it is straightforward to calculate $c_{DE}(x,t)$. In Fig. 2 we show $c_{DE}(x,t)$ as a function of x for the same times t used in Fig. 1 ($n\sigma^3 = 0.5$). Although $c_{DE}(x,t)$ has all the same qualitative features of the simulation results shown in Fig. 1, the diffusion equation solution spreads too rapidly. That is, at very short times the mass flux is too large. The explicit solution for $j_{1DE}(x,t)$ shows that $j_{1DE} \propto t^{-1/2}$ (as $t \to 0$) at the edge of the initial rectangular pulse, a well-known but often ignored problem.

The damped wave equation

In the initial (very short time) stage the mixing of species 1 and 2 is caused by the free streaming of all particles. In this limit $j_1 \propto (k_BT/m)^{1/2}$ at the edge of the initial pulse -- i.e. j_1 is a finite constant as $t \to 0$. A damped wave equation in which the propagation speed is the thermal velocity will correctly describe this earliest phase of the mixing. By making the damping constant proportional to D, such an equation will approach the diffusion equation as $t \to \infty$. Maxwell [1], and subsequently many others [4], have argued that this type of equation, which also has the feature that the initial condition cannot propagate faster than the wave speed, should replace the parabolic hydrodynamic equations (the diffusion and heat equations). The Telegrapher's equation

$$\frac{1}{u^2}\frac{\partial^2 c_{TE}}{\partial t^2}+\frac{1}{D}\frac{\partial c_{TE}}{\partial t}=\frac{\partial^2 c_{TE}}{\partial x^2} \quad , \tag{2}$$

where u is the wave speed, is the most frequently studied equation of this type. With u = $(k_B T/m)^{1/2}$ the solutions of Eq. (2) have some features of the correct behavior in the $t \to 0$ and $t \to \infty$ limits. However, as can be seen in Fig. 3, the solution $c_{TE}(x,t)$ does not bear much qualitative resemblance to the simulation results. In particular $c_{TE}(x,t)$ shows distinct wave fronts and a wake that do not appear in the simulation results.

Generalized hydrodynamics

By making a small change in the form of the expansion method used in generalized hydrodynamics we showed in Ref. [3] that it was possible to avoid the use of partial differential equations to describe self-diffusion:

$$c_{GH}(x,t)=\sum_{i=1}^{\infty} c^{(i)}(x,t) \quad , \tag{3}$$

with the first three $c^{(i)}$ given by

$$c^{(1)}(x,t)=\int dx' G_K(x-x')c(x',0) \quad , \tag{4}$$

$$c^{(2)}(x,t)=\frac{\rho_2(t)}{4\rho_1(t)^2}\int dx' G_K(x-x')\left[4w^4-12w^2+3\right]c(x',0) \quad , \tag{5}$$

$$c^{(3)}(x,t)=\frac{\rho_3(t)}{8\rho_1(t)^3}\int dx' G_K(x-x')\left[8w^6-60w^4+90w^2+15\right]c(x',0) \quad . \tag{6}$$

Here $w=(x-x')/\sqrt{4\rho_1(t)}$ and $G_K(x-x')=\exp\left[-w^2\right]/\sqrt{4\pi\rho_1(t)}$.

The first term on the right hand side of Eq. (3), $c^{(1)}(x,t)$, is a solution of the diffusion equation with a time dependent diffusion coefficient $D(t) = \partial\rho_1/\partial t$. In the limit $t \to 0$

$c_{GH}(x,t)$ reduces to the correct free streaming result, and as $t \to \infty$, $c_{GH} \to c_{DE}$ for $d > 2$. (Recall that for d=2 the diffusion coefficient does not exist.) Since the ratios ρ_i/ρ_1^i appear to be quite small for all times, Eq. (3) seems ideally suited to describe all stages of self diffusion for any dimensionality d [3].

In Figs. 4-6 we compare c_{MD} to c_{DE} , $c^{(1)}$, and the third approximation to c_{GH}, $c_{GH}^{(3)} = c^{(1)} + c^{(2)} + c^{(3)}$. [For d=2, $n\sigma^3=0.5$ we chose $D=0.475\ \sigma(\varepsilon/m)^{1/2}$.] Let $\Delta = c_{GH}^{(3)} - z(x,t)$, where z(x,t) is c_{MD} (the crosses) or c_{DE} (curve a) or $c^{(1)}$ (curve b). $c_{GH}^{(3)} - c_{MD}$ does not differ significantly from zero over the entire range of x and t considered in this study and $c^{(1)}(x,t)$ is found to be an excellent approximation over this range.

SYMBOLS

d	system dimensionality
ε	Lennard-Jones energy parameter
σ	Lennard-Jones distance parameter
N	number of particles
V	system volume
L_x	system length in x-direction
L_p	system length normal to the x-direction
k_B	Boltzmann's constant
T	temperature
$<...>_{MD}$	average over a trajectory

t	time
x	x-coordinate
m	particle mass
$d(t)$	single-particle displacement
$c(x,t)$	mole fraction of species 1
N_I	number of initial states
n	N/V
$\rho_i(t)$	i-th cumulant of d(t)
j_1	number flux of species 1
D	self-diffusion constant
u	wave speed
Δ	mole-fraction difference

REFERENCES

[1] J. Clerk Maxwell, Phil. Trans. R. Soc. London, 157 (1867) 49-88.

[2] W. W. Wood and J. J. Erpenbeck, J. Stat. Phys, 27 (1982) 37-56.

[3] J. M. Kincaid, Phys. Rev. Letts., 74 (1995) 2985-2988.

[4] D. Jou, J. Casas-Vazquez, and G. Lebon, Rep. Prog. Phys., 51 (1988) 1105-1132; D. D. Joseph and L. Preziosi, Rev. Mod. Phys., 61 (1989) 41-75 and 62 (1990) 375-393.

[5] B. L. Holian and D. J. Evans, J. Chem. Phys., 78 (1983) 5147-5150.

[6] J. M. Kincaid, R-F. Tuo, and M. Lopez de Haro, Mol. Phys., 81 (1994) 837-850.

[7] V. F. Sears, Phys Rev., A5 (1972) 452-462; I. M. de Schepper, M. H. Ernst, and E. G. D. Cohen, J. Stat. Phys., 25 (1981) 321-360; I. M. de Schepper and M. H. Ernst, Physica (Amsterdam), 98A (1979) 189-214.

FIGURE CAPTIONS

Fig. 1 Molecular dynamics calculations of $c_{MD}(x,t)$ as a function of x for times t* = 0, 0.54,1.08,1.62, 2.16, and 2.70. ($t = t^*\sigma(m/\varepsilon)^{1/2}$, d=3, $n\sigma^3 = 0.5$)

Fig. 2 Solution of the diffusion equation, $c_{DE}(x,t)$, as a function of x for times t* = 0, 0.54,1.08,1.62, 2.16, and 2.70. ($t = t^*\sigma(m/\varepsilon)^{1/2}$, d=3, $n\sigma^3 = 0.5$)

Fig. 3 Solution of the Telegrapher's equation, $c_{TE}(x,t)$, as a function of x for times t* = 0, 0.54,1.08,1.62, 2.16, and 2.70. ($t = t^*\sigma(m/\varepsilon)^{1/2}$, d=3, $n\sigma^3 = 0.5$)

Fig. 4 Comparison of c_{MD} (crosses), c_{DE} (a), and $c^{(1)}$ (b) to $c_{GH}^{(3)}$. ($t = 1.08\ \sigma(m/\varepsilon)^{1/2}$, d=3, $n\sigma^3 = 0.5$)

Fig. 5 Comparison of c_{MD} (crosses), c_{DE} (a), and $c^{(1)}$ (b) to $c_{GH}^{(3)}$. ($t = 0.54\ \sigma(m/\varepsilon)^{1/2}$, d=3, $n\sigma^3 = 0.2$)

Fig. 6 Comparison of c_{MD} (crosses), c_{DE} (a), and $c^{(1)}$ (b) to $c_{GH}^{(3)}$. ($t = 1.2\ \sigma(m/\varepsilon)^{1/2}$, d=2, $n\sigma^2 = 0.5$)

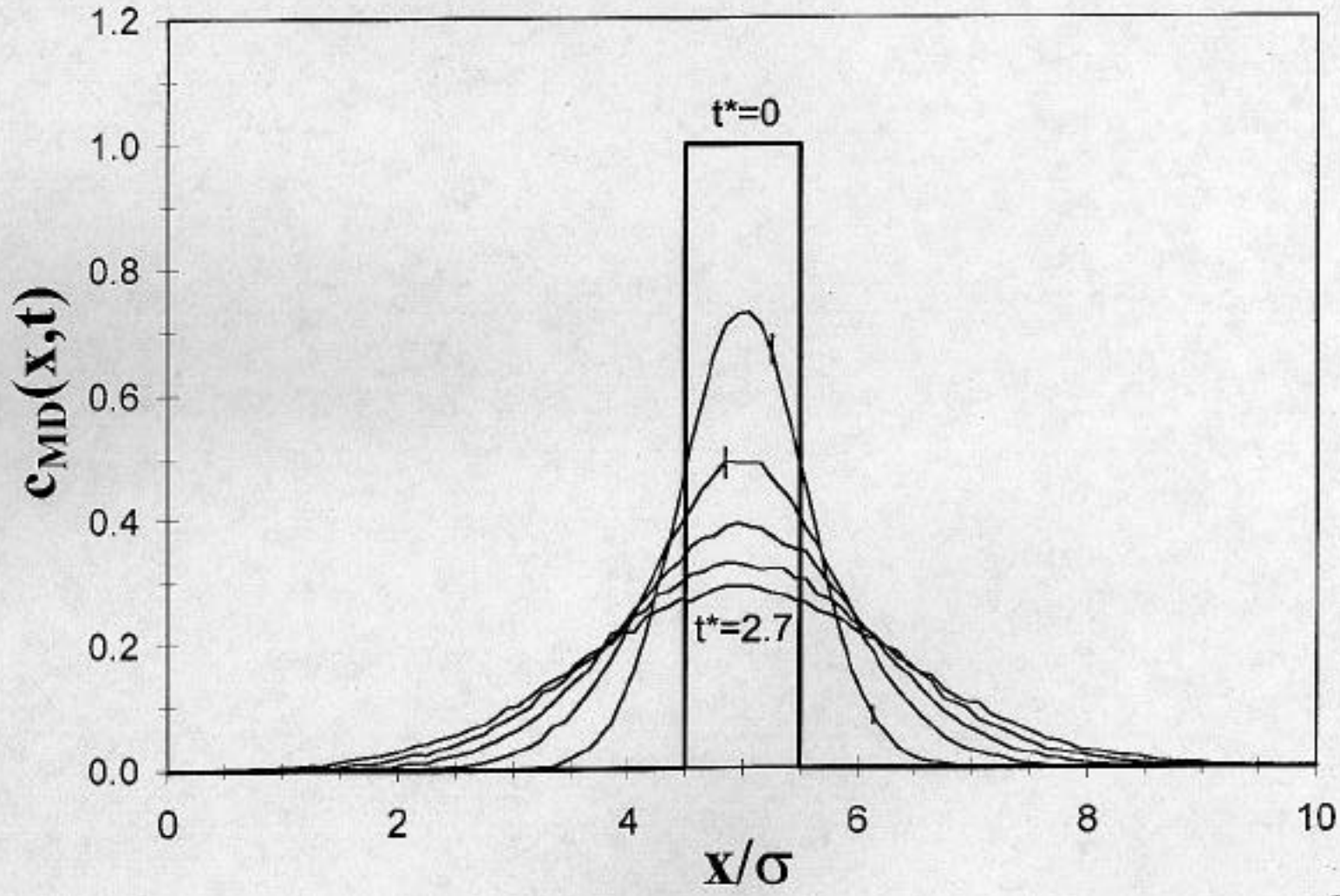

Fig. 1

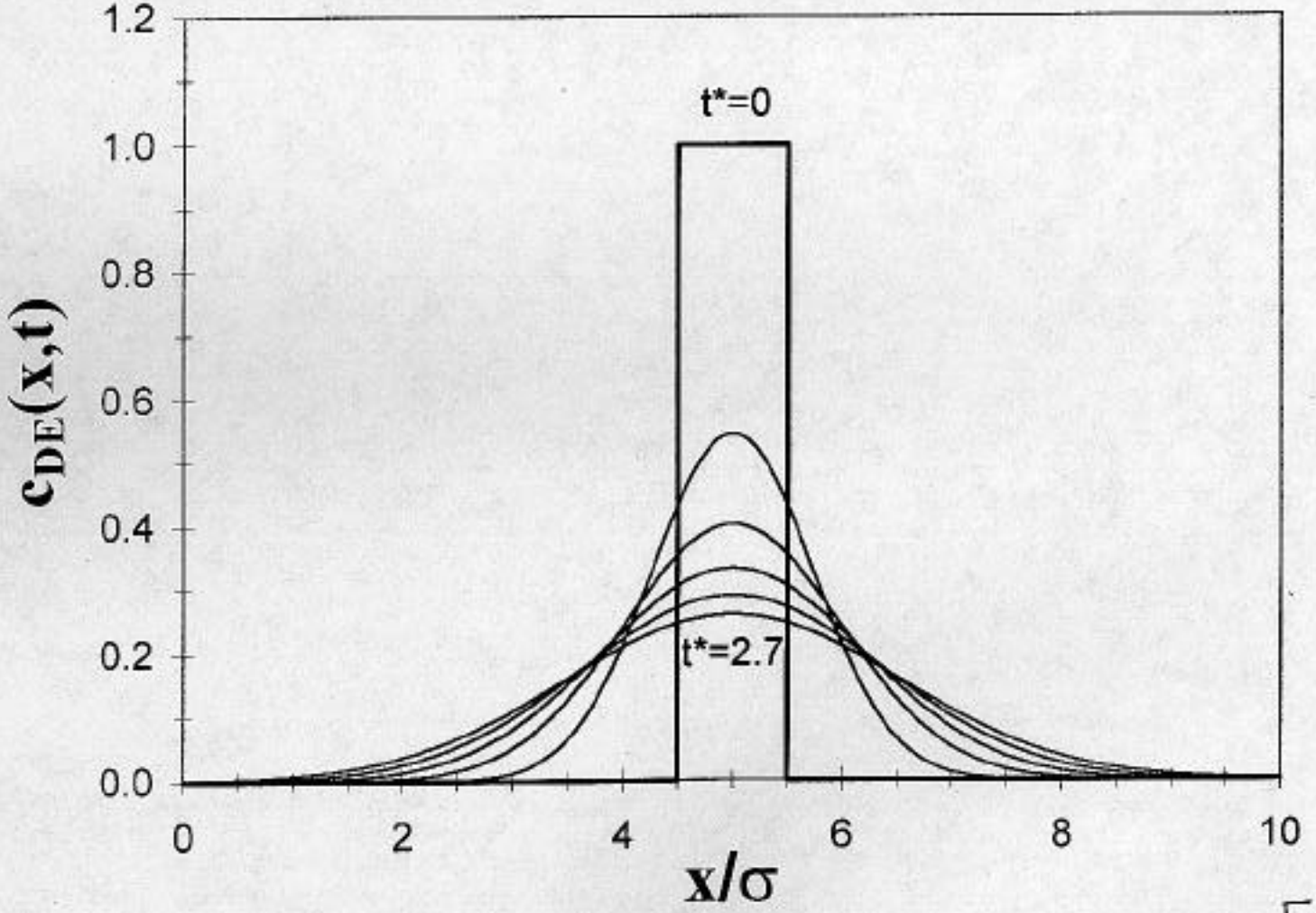

Fig. 2

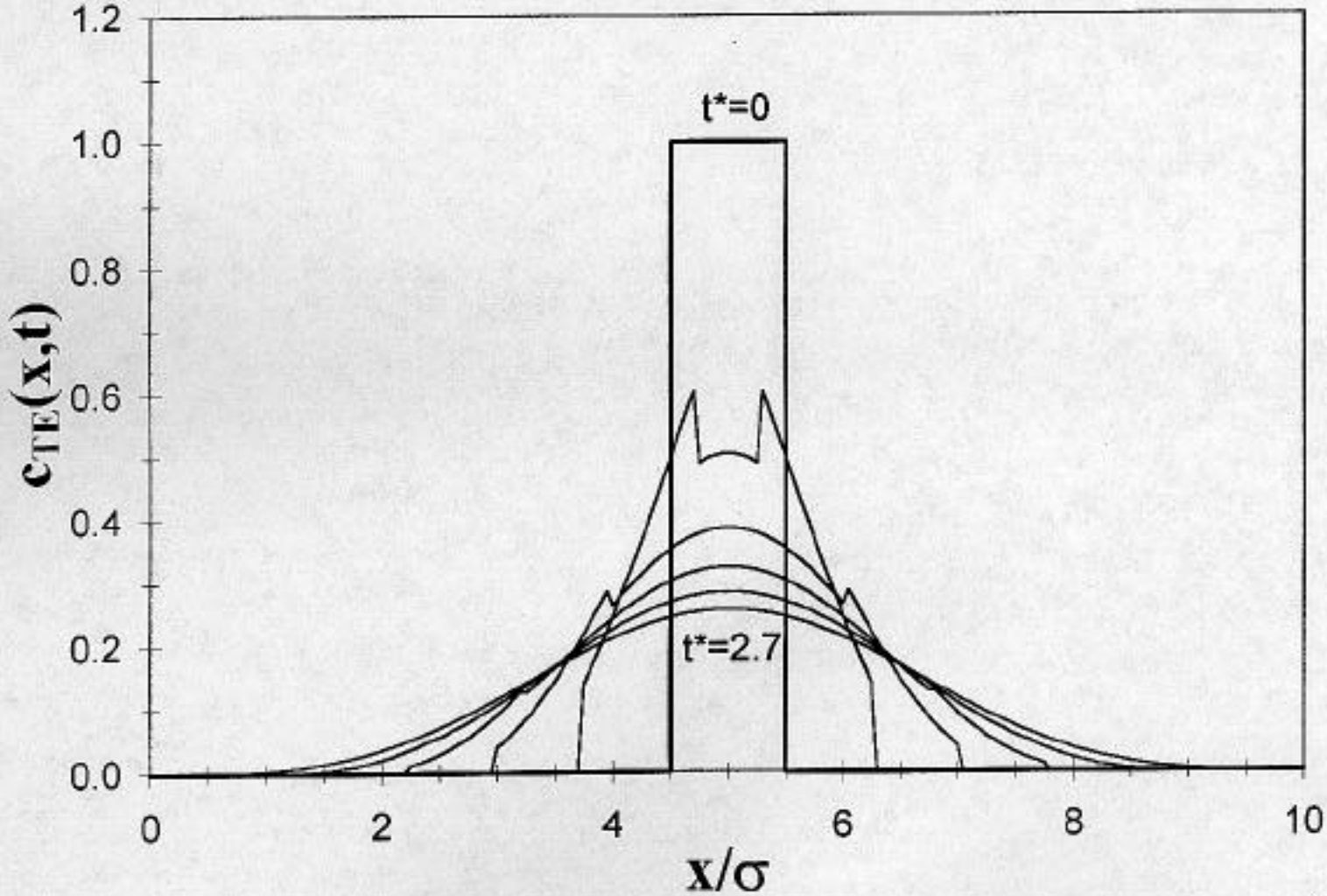

Fig. 3

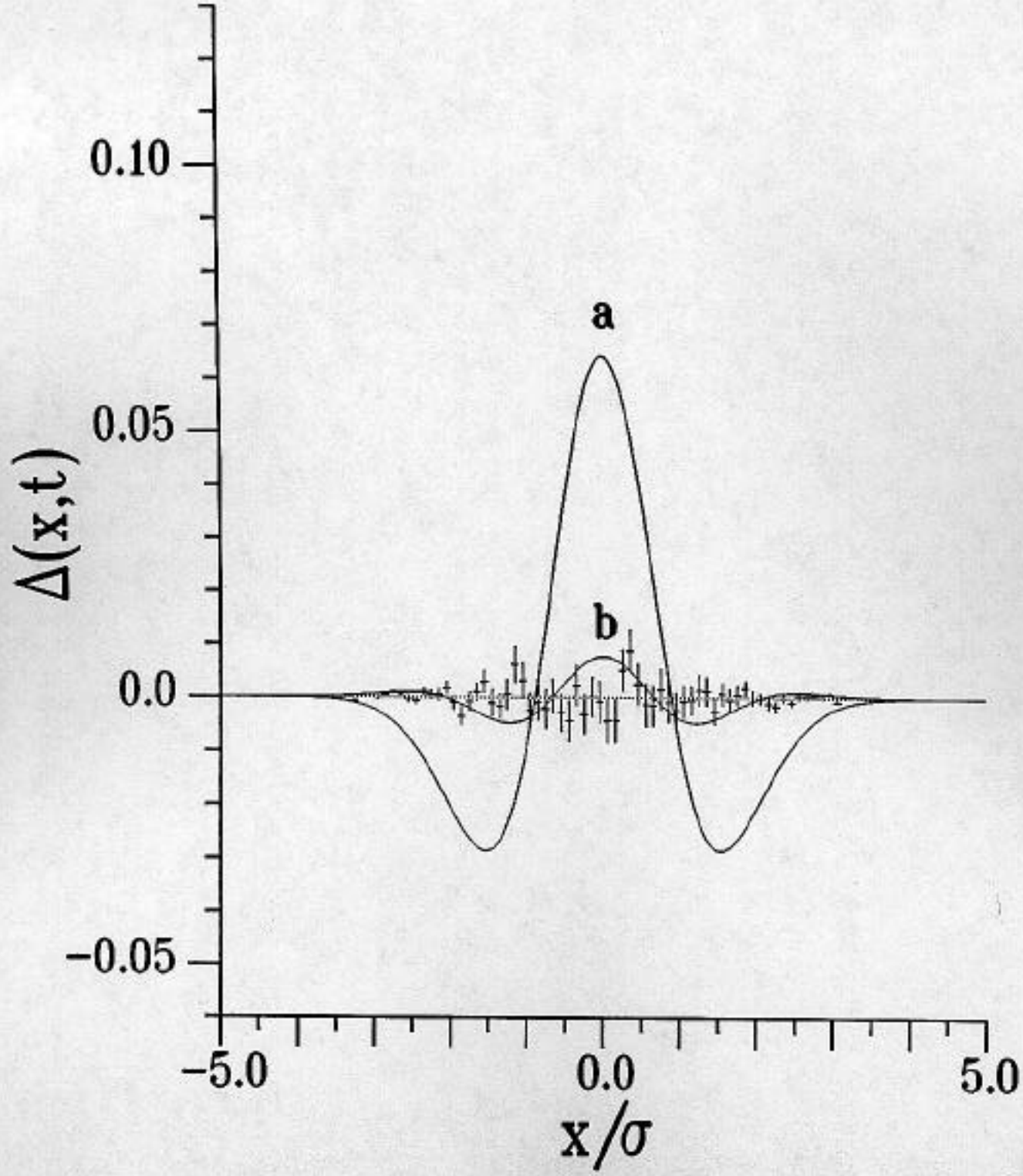

Fig. 4

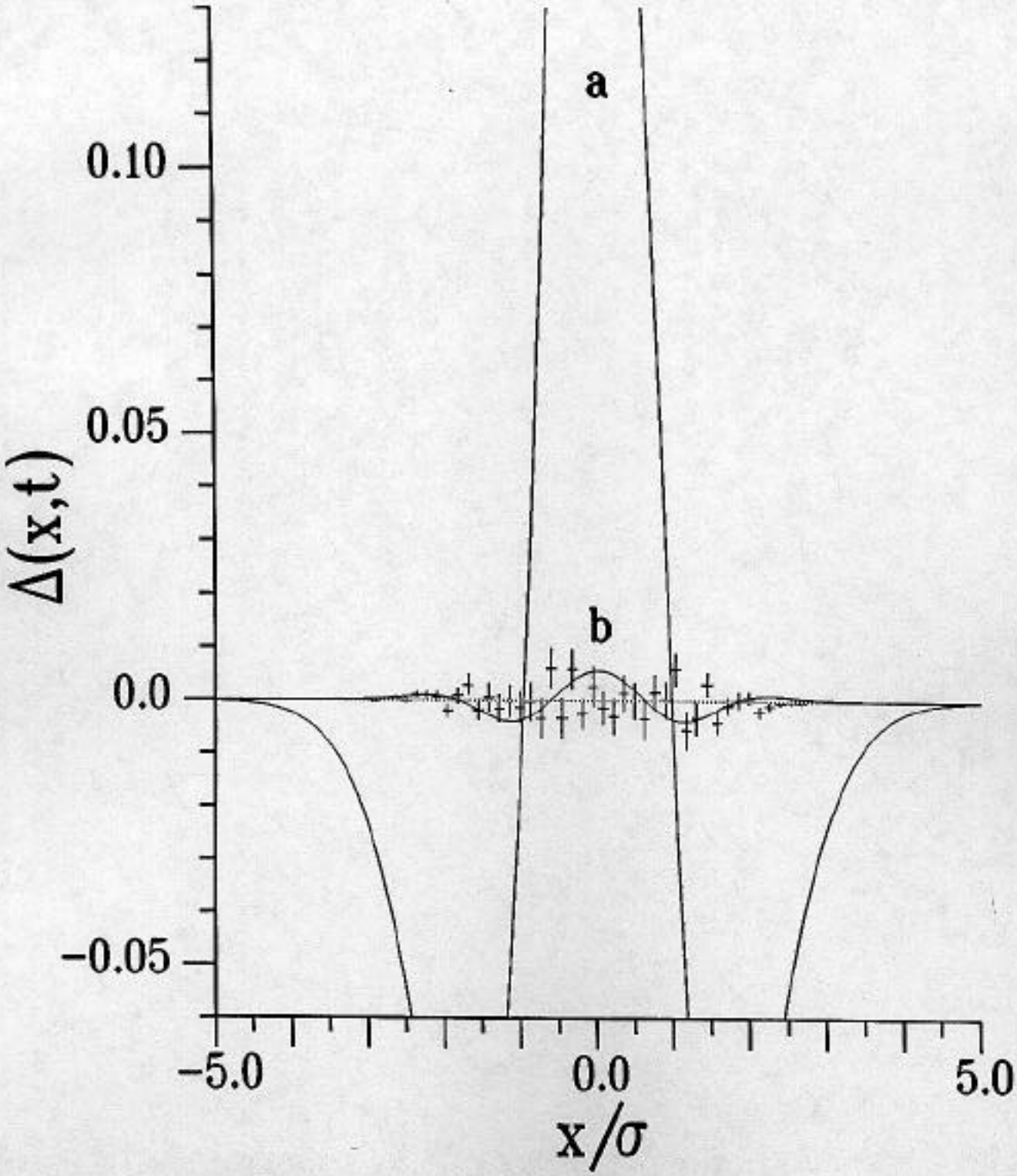

Fig. 5

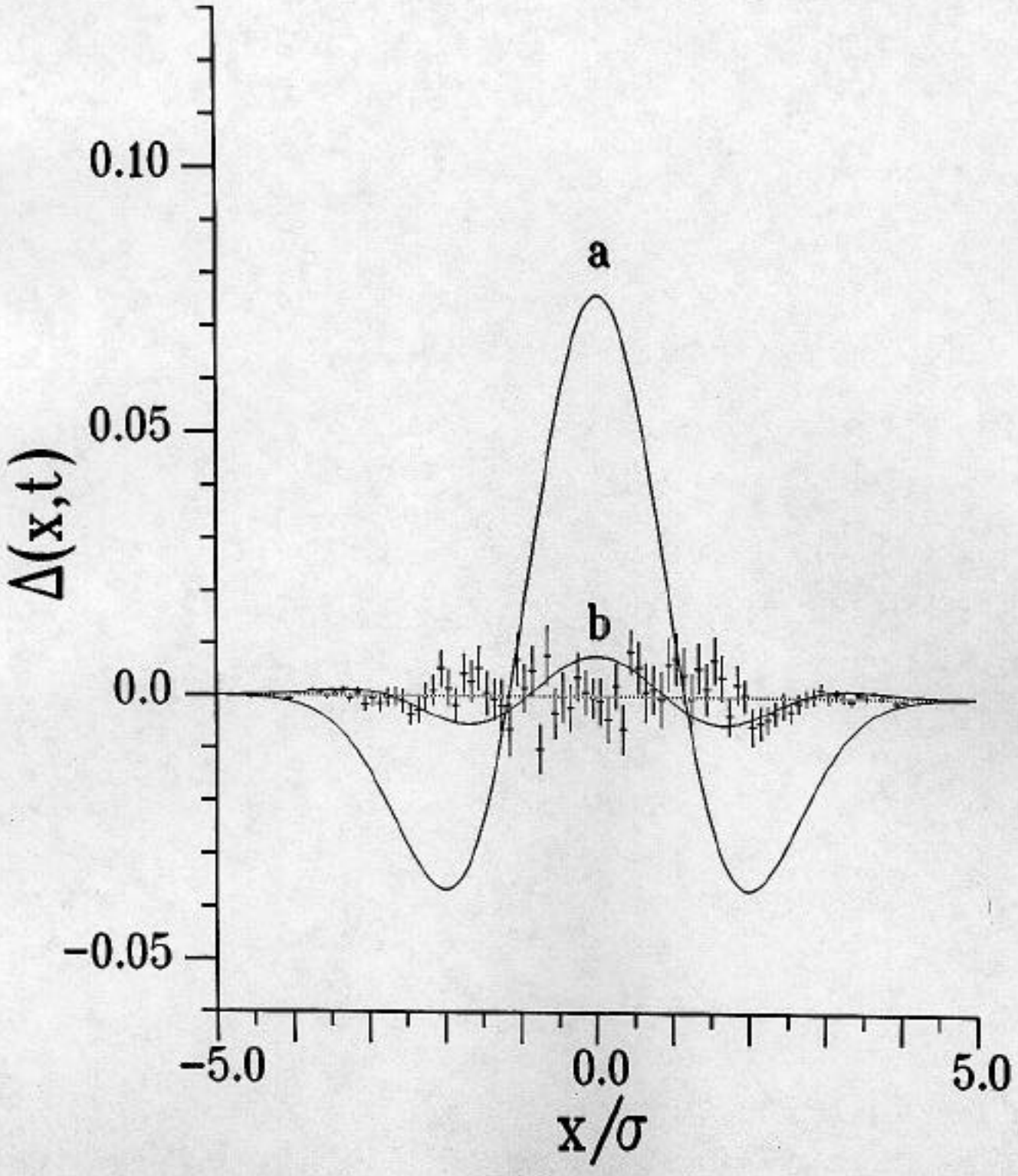

Fig. 6